LAWRENCE
LIVERMORE
NATIONAL
LABORATORY

LLNL-TR-509672

Meteorological Observations for Renewable Energy Applications at Site 300

S. Wharton, M. Alai, K. Myers

October 31, 2011

Disclaimer

This work performed under the auspices of the U.S. Department of Energy by Lawrence Livermore National Laboratory under Contract DE-AC52-07NA27344.

Meteorological observations for renewable energy applications at Site 300

Project team: Sonia Wharton, Maureen Alai, Cary Gellner, Katie Myers, Jeff Mirocha, John van Fossen

1. Overview

In early October 2010, two Laser and Detection Ranging (LIDAR) units (LIDAR-96 and LIDAR-97), a 3 m tall flux tower, and a 3 m tall meteorological tower were installed in the northern section of Site 300 (Figure 1) as a first step in development of a renewable energy testbed facility. This section of the SMS project is aimed at supporting that effort with continuous maintenance of atmospheric monitoring instruments capable of measuring vertical profiles of wind speed and wind direction at heights encountered by future wind power turbines. In addition, fluxes of energy are monitored to estimate atmospheric mixing and its effects on wind flow properties at turbine rotor disk heights. Together, these measurements are critical for providing an accurate wind resource characterization and for validating LLNL atmospheric prediction codes for future renewable energy projects at Site 300.

Accurate, high-resolution meteorological measurements of wind flow in the planetary boundary layer (PBL) and surface-atmosphere energy exchange are required for understanding the properties and quality of available wind power at Site 300. Wind speeds at heights found in a typical wind turbine rotor disk (~ 40- 140 m) are driven by the synergistic impacts of atmospheric stability, orography, and land-surface characteristics on the mean wind flow in the PBL and related turbulence structures. This section of the report details the maintenance and labor required in FY11 to optimize the meteorological instruments and ensure high accuracy of their measurements. A detailed look at the observations from FY11 is also presented. This portion of the project met the following milestones:

Milestone 1: successful maintenance and data collection of LIDAR and flux tower instruments
Milestone 2: successful installation of solar power for the LIDAR units
Milestone 3: successful implementation of remote data transmission for the LIDAR units

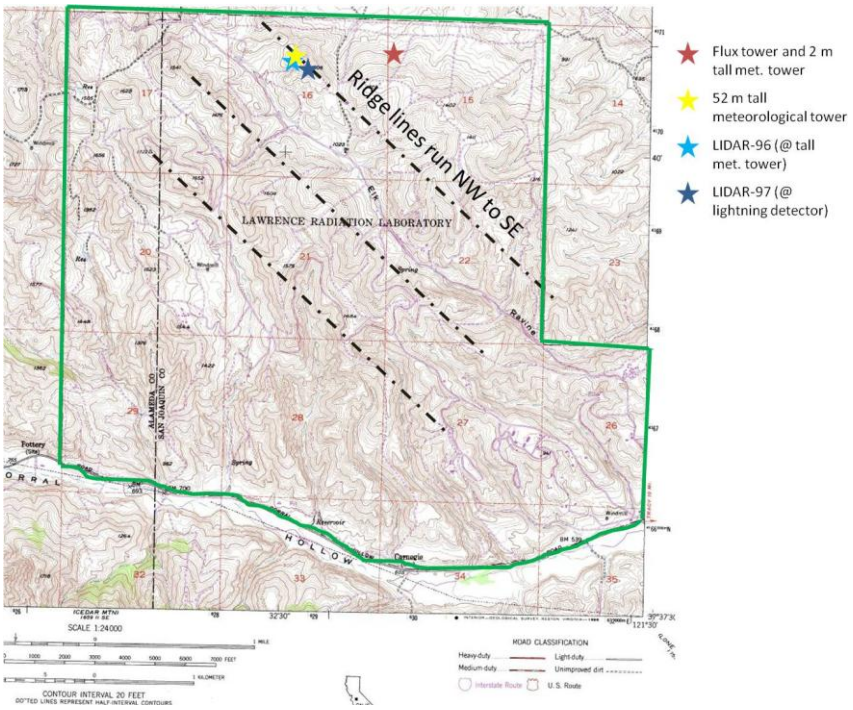

Figure 1: Topographical map of Site 300 showing the locations of the flux tower and 3 m meteorological tower (37.675, -121.531, 323 m AGL), LIDAR-97 (37.674, -121.540, 398 m AGL), LIDAR-96 (37.675, -121.541, 387 m AGL), and the existing 52 m tall meteorological tower (37.675, -121.541, 387 m AGL). Also shown are the dominant ridge lines (dashed lines) which run northwest-to-southeast across Site 300. The flux tower and LIDARs are separated by a distance of 1 km; the LIDARs are separated by a distance of 150 m.

2. Instrument maintenance and data collection

The success of this observational network was largely attributed to close collaborations between Site 300 staff and SMS project scientists, between IWS staff (mostly in Global Security) and SMS project scientists, and frequent contact between project scientists and the instrument manufacturers, Campbell Scientific, Inc. and NRG Systems, Inc. Coordination between Site 300 staff and the project scientists was required to obtain permission and extra labor for the LIDAR relocations, digging permits for the LIDAR antennae (for remote data transmission), and for solar panel installations at the LIDARs. This project's IWS required two revisions as new tasks were added to include the solar panel installation. It is important to stress that obtaining accurate measurements either from the LIDAR units, flux tower, or 3 m tall meteorological tower with minimal data loss requires weekly visual checks and routine maintenance as these instruments are exposed continuously to weather and animal hazards. Instrument details are listed in Table 1. Photographs of each tower and LIDAR unit are found in Figure 2.

Instrument	Location	Variables measured	Sampling height(s)	Sampling rate	Averaging time	Power source
LIDAR-96	@ 52 m tall met. tower	wind speed, wind direction, turbulence	40-200 m, every 20m	1 Hz	10 minutes	grid power until June, then solar
LIDAR-97	@ lightning detector	wind speed, wind direction, turbulence	40-200 m, every 20m	1 Hz	10 minutes	grid power until June, then solar
sonic anemometer & infrared gas analyzer	flux tower	sensible heat flux, latent heat flux, specific humidity, air temperature, wind speed, wind direction, turbulence	2 m	10 Hz	30 minutes	solar
net radiometer	flux tower	net radiation	2 m	1 Hz	30 minutes	solar
temperature/relative humidity probe	3 m tall met. tower	air temperature & relative humidity	2 m	1 Hz	30 minutes	solar
cup anemometer & wind vane	3 m tall met. tower	wind speed and direction	2 m	1 Hz	30 minutes	solar

Table 1: List of instruments maintained during this project and their associated measurements including sampling height, rate, and averaging time. Note that LIDAR-97 was moved to the 52 m tall met. tower in February and March while LIDAR-96 was at the manufacturer for repairs. LIDAR-96 is currently in South Dakota for a DOE EERE wind forecasting project (since June 2011). The LIDARs and towers are mobile systems.

All of the instruments were checked weekly by Sonia Wharton to ensure that they were working properly and to look for bird or rodent damage as the equipment are located in remote, wildlife-rich areas. Sonia Wharton, Maureen Alai, Jeff Mirocha, and Katie Myers were trained on how to maintain and download data from the LIDARs. In addition, Sonia trained Katie on how to maintain and download data from the flux and 3 m tall meteorological towers. The flux and short meteorological towers required weekly trips for data collection via a laptop to datalogger connection for data downloading. During the rainy season, the flux tower required hiking ~2 km as the roads became impassible. Off-road permission was always established and safety protocols were followed. The LIDARs initially required data collection with a laptop via an Ethernet cord connection. This was done weekly. Starting in May 2011, remote data collection was made possible via a modem/cell phone service connection. Each week, 1 Hz and 10 minute-averaged observations were downloaded from the LIDARs, 10 Hz and 30-minute

observations were downloaded from the flux tower, and 30 minute-averaged observations were downloaded from the 3 m tall meteorological tower. All data were archived on multiple computers as well as stored on a shared network server. Data were screened each week for outliers and missing values to ensure that the instruments were working correctly.

Figure 2: Meteorological instrumentation at Site 300 for the renewable energy program includes (a) LIDAR-96 co-located with the tall meteorological tower at the East Observational Point (EOP), (b) LIDAR-97 near the lightning detector at the EOP, and (c) 3 m tall meteorological and energy flux towers in the valley below. The LIDARs are located on a ridgeline west (and usually upwind) of the flux tower.

Remote data access made it possible to check the status of the LIDAR units daily from the main LLNL campus. This greatly reduced instrument downtime as a LIDAR could be visited and fixed the following day if a problem was detected. In nearly all cases, restarting the LIDAR units manually fixed any data collection problems. LIDAR-96 proved to be more problematic than LIDAR-97 and was sent back to NRG twice for repairs. The first repair fixed an issue with the laser and the second repair fixed the laser window which had become damaged by the wiper fluid (we used the fluid recommended by the manufacturer but they later discovered problems with it). Routine once-a-week maintenance at the LIDARs included keeping the glass windows clean and checking the signal to noise ratio, laser strength, compass orientation, pitch/roll angles, and alarm files to ensure that the units were working properly. In FY11, data availability was 74% from LIDAR-96 (data gaps mostly due to downtime when the instrument was repaired at NRG) and 67% from LIDAR-97 (data gaps mostly due to downtime in March and April when we had plans to send the unit back to NRG for software updates and lower data availability in July and August when the signal to noise ratio started degrading). LIDAR-97 will be sent back to NRG for repairs at the end of FY11 as the problem is internal to the unit and cannot be fixed onsite. The LIDARs are reliant on aerosols in the atmosphere to backscatter radiation back to the unit. We found that the percentage of data availability dropped significantly above 160 m, most likely because the atmosphere was “too clean” which caused the signal-to-noise ratio (SNR) to be too low for data recovery.

Routine maintenance of the flux tower and 3 m tall meteorological tower included checking the infrared red gas analyzer (IRGA) signal strength, checking voltages to make sure that the instruments never received less than 12 V DC, checking the bubble level on the sonic anemometer to make sure the instrument was always level relative to the ground, checking for error flags in the data records, and checking the status of the dataloggers to make sure they were collecting and storing data properly. Initially the flux tower had a problem with large birds landing on the instruments and instrument booms. We added bird spikes in November and the problem was fixed. The IRGA had to be returned to

Campbell Scientific, Inc. in May for repairs. A glitch in the instrument's operating system removed the instrument's calibration files and a remote instrument repair could not be made even after several attempts to reinstall the files. The instrument was fixed at Campbell Scientific, Inc. and a lower availability of flux data compared to the 3 m tall meteorological tower is due to this repair downtime. In FY11, data availability was 98% from the 3 m tall meteorological tower and 78% from the flux tower.

3. Observations

3a. Comparison of co-located LIDAR and tall meteorological tower wind speed and direction

We utilized the existing 52 m tall meteorological tower to check the accuracy of wind speed and direction at a co-located height from the LIDARs. The tall meteorological tower is equipped with cup anemometers and wind vanes at heights of 10, 23, and 52 m above ground level. The closest height in common was 60 m from the LIDARs. The tall meteorological tower had an averaging time of 15 minutes while the averaging time for the LIDARs was 10 minutes. Because of this all data are shown as hourly averages. Even with the slight mismatches between measurement height and averaging times, the correlations between the LIDARs and tall meteorological tower were very high. LIDAR measurements of hourly average wind speed were nearly identical to the wind speed measured by the tall meteorological tower. Data for LIDAR-97 are shown in Figure 3 for the months of February and March. The few outliers are likely due to a combination of slightly different averaging times between the instruments and very gusty conditions. February and March are presented because they are gustier months and represent periods with a lower fit between the two sets of observations. The R-square value for the other months is ~0.98.

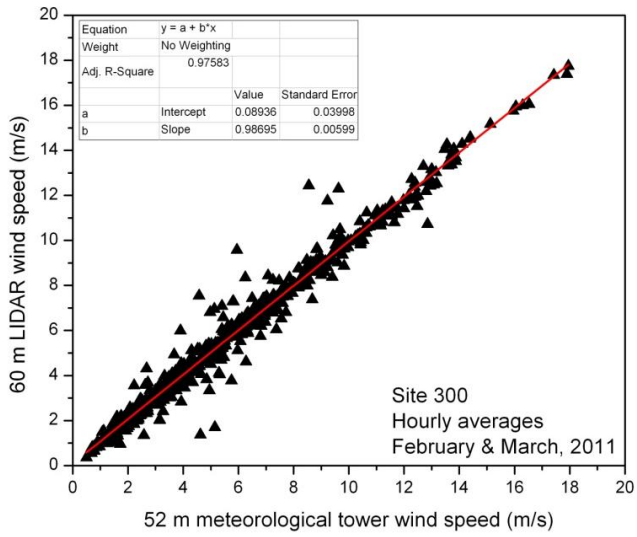

Figure 3: Hourly average wind speed at 60 m from the co-located LIDAR-97 and at 52 m from the tall meteorological tower show high correlation between the independent datasets in February and March, 2011. The data were fit with a linear regression model (R-square = 0.976, slope = 0.989) and closely resemble a 1:1 line.

High correlations between wind direction measured by the LIDAR (at 60 m) and tall meteorological tower (at 52 m) were also found. Figure 4 indicates that both LIDAR-97 and the tall

meteorological tower measured winds primarily from the northwest direction in autumn and winter with secondary peaks in the southeasterly and southwesterly directions. During the summer, both instruments show that the winds were predominantly from the southwest or westerly directions. The most infrequent wind directions were from the northeast and east and occurred less than 10% of the year.

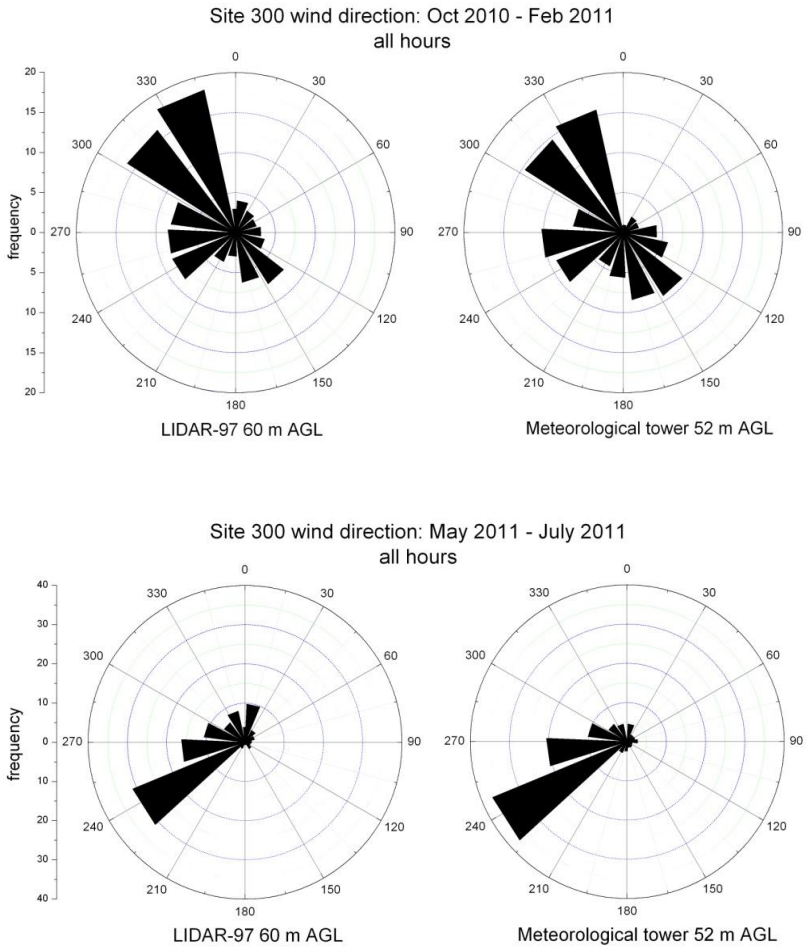

Figure 4: Histogram of wind direction by season and instrument shows good correlation between the co-located LIDAR-97 and tall meteorological tower. Wind direction in the autumn and winter is predominantly from the northwest while winds shift to the southwest in the late spring and summer.

3b. LIDAR observations: seasonal and diurnal wind shear patterns

Continuous data collection up to 200 m from the LIDARs allowed us to quantify the wind speed profile above the EOP ridgeline. Wind flow at these heights is indicative of the amount of kinetic energy that would be available to wind turbines for power production. We observed distinct seasonal and diurnal wind speed patterns at this location as shown in Figure 5. Maximum winds were measured during the warm, dry season and minimal winds during the cool, wet season. This is consistent with other inland locations near the Bay Area. When wind speed was analyzed by height, distinct patterns in wind shear became apparent. In the winter months, wind speed generally increased with height (i.e.,

positive shear) as is generally expected. During times of positive shear, frictional drag causes the wind speed to become zero close to the ground while the pressure gradient forces cause the wind to increase with height. In contrast, periods of strong negative shear (i.e., wind speed decreasing with height) were observed during the spring and summer months. Negative shear was the strongest during the nighttime hours although it also occurred during the day. For example, on July nights, the wind speed at 40 m above the surface was more than 3 m/s faster than the wind speed at 140 m (Figure 5b).

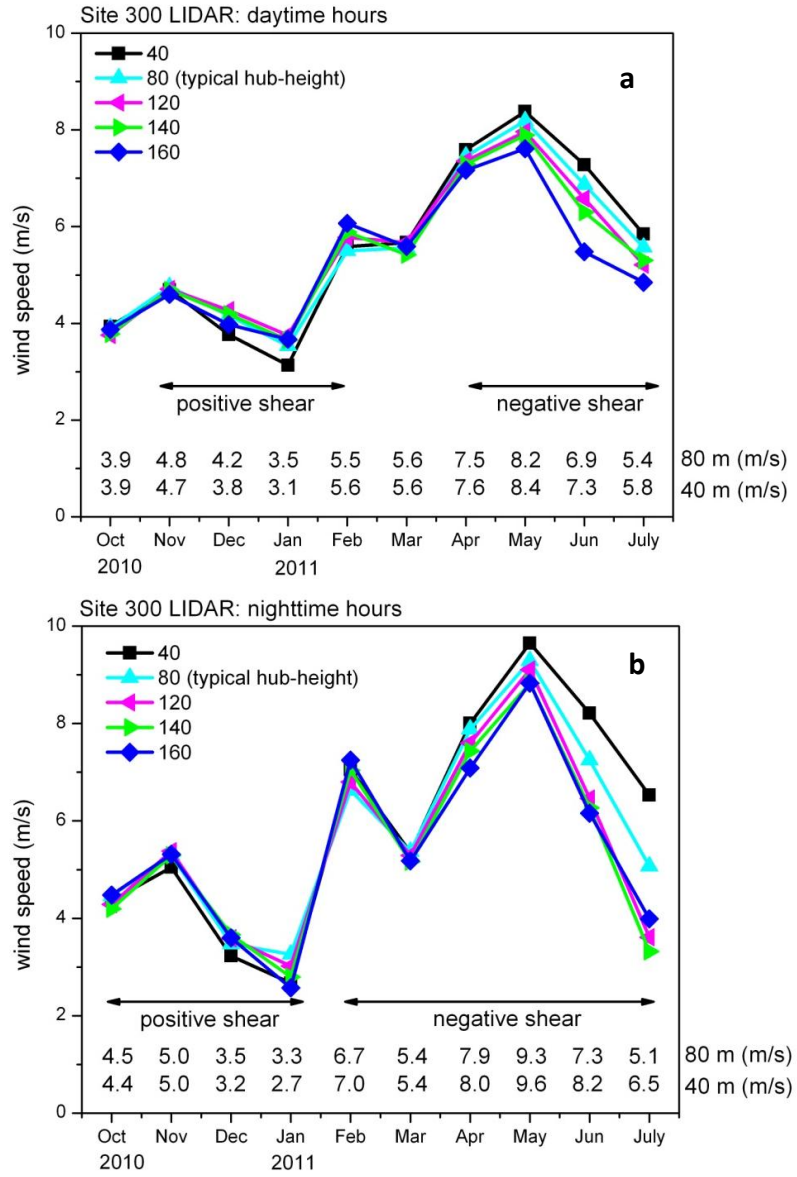

Figure 5: Monthly mean wind speed during (a) daylight and (b) nighttime hours at the LIDARs from 40 m to 160 m above ground level. Also shown are the monthly averages for the 40 m and 80 m heights. Average wind speeds peak in May and are slowest in January and generally are higher at night than during day. Positive wind shear is observed in November-February while negative shear dominates from March-July.

Figure 6 shows vertical profiles of wind speed normalized by a typical turbine hub-height (the 80 m wind speed). Normalizing wind speed shows whether wind in the upper portion of a wind turbine

would be greater or less than wind in the lower portion of the turbine. For example, during periods of positive shear, the upper half of a rotor disk would experience greater wind speeds than found at hub-height or in the lower half of the disk. In Figure 6, the theoretical wind speed profile is plotted based on the log law,

$$U(z) = (\frac{u_*}{k}) \ln(\frac{z}{z_o}) \quad (1)$$

In Eq (1), U(z) is mean wind speed (m/s) at height z (m), u_* is friction velocity (m/s) or the momentum fluxes, k is the von Karman constant (0.4), and z_o is the canopy roughness length. Friction velocity was based on measurements of the momentum fluxes at the flux tower and z_o was based on average canopy roughness length values found in the literature for a grassland canopy. In Figure 6 it is apparent that over this ridge line negative shear is usually the strongest between heights of 23 m and 60 m. Overall, strongest negative shear was observed in May and June and during the nighttime hours. At night, peak winds occurred at 23 m above the surface in all months except for November and December. Peak daytime winds occurred farther above the surface, ranging from 40 m in October and March-June to 120 m in December-January. The maximum wind resource at this ridge line was nearer to the ground than predicted by the log law. This was particularly true at night and a strong bulge in the wind speed is frequently apparent at heights of 10-40 m AGL (Figure 6). With regard to mean flow (i.e., disregarding turbulence) it appears that wind turbines at Site 300 would benefit from accessing these maximum velocity flows 30-60 m above the surface.

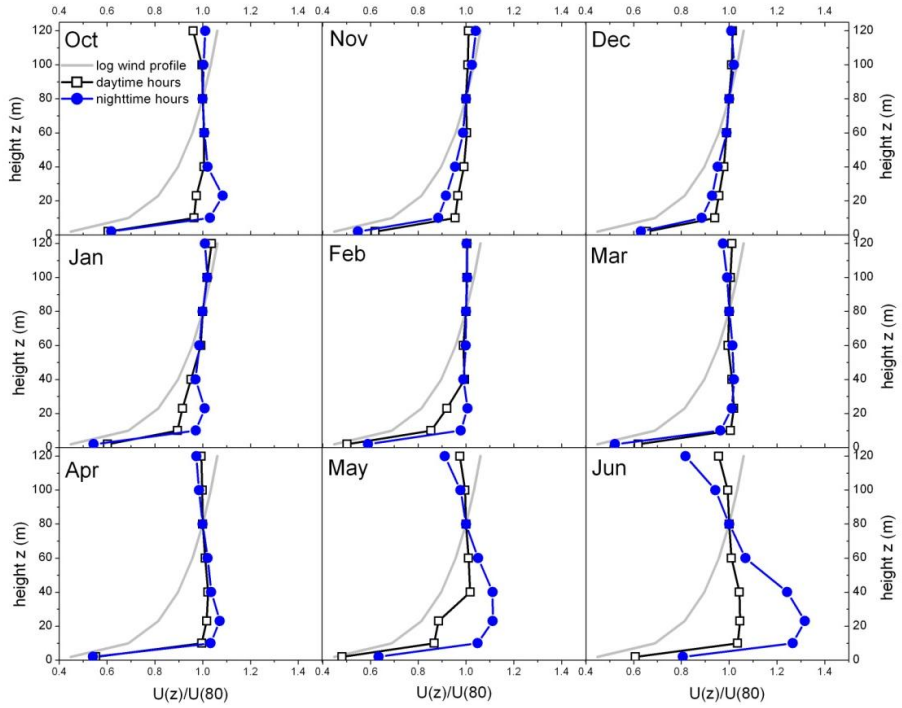

Figure 6: Monthly mean vertical profiles of wind speed normalized by the 80 m wind speed (typically hub-height) during daytime (open squares) and nighttime hours (closed circles). Wind speed measurements at 40-120 m above ground level are from the LIDARs, 23 and 10 m are from the tall meteorological tower, and 2 m is from the flux tower. Also plotted is the theoretical wind profile according to the log law (solid gray line).

3c. LIDAR observations: wind shear induced by complex terrain

The log law represents wind conditions that one would expect over flat terrain during neutral stability. Although these conditions are only occasionally met, the log law is still utilized by wind farm developers to predict wind speeds aloft when measurements above a tall meteorological tower are not available. The effects of complex terrain on wind flow are rarely carefully studied and thus poorly understood. Site 300 provides an excellent test site to study the impacts of complex terrain on wind flow for renewable energy applications as the site has numerous upwind and downwind ridge lines, steep canyons, and valleys (Figure 7) and the meteorological instrumentation were designed to be mobile.

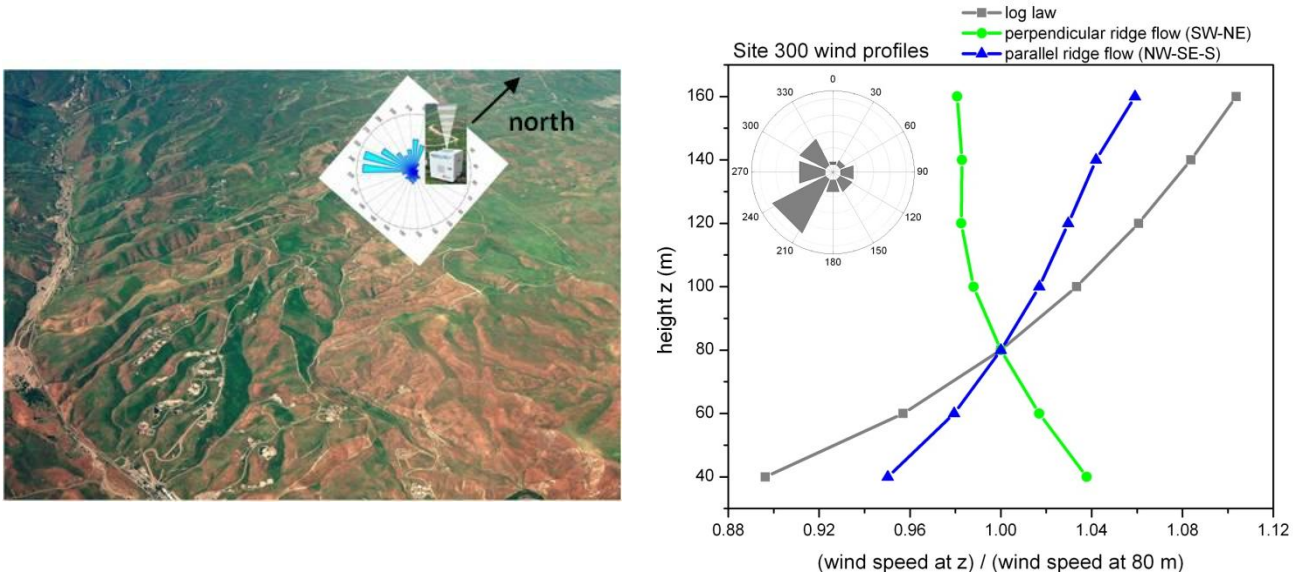

Figure 7: (left) Aerial photograph of Site 300 showing the complex terrain and northwest-to-southeast orientation of the ridge lines. LIDAR-96 is located in the northern section of Site 300 and the annual wind rose shows that the winds are predominately from the southwest or from the direction perpendicular the major ridge lines. (right) Vertical profile of mean wind speed observations normalized by the 80 m measurement height as a function of wind direction. Shown here are the wind speed profiles during times of perpendicular ridge flow (winds from the SW or NE) and during times of parallel ridge flow (winds from the NW, SE or S). The log law is plotted to show what a typical wind profile might look over flat terrain to illustrate the effects of terrain on wind shear at Site 300.

3d. Flux tower observations: energy exchange between the surface and atmosphere

Canopy height (i.e., canopy roughness) and vegetation "greenness" affect atmospheric mixing and wind shear in a couple of way. First, the height and density of the canopy changes the sizes of mechanically-produced turbulent eddies which are the primary producers of turbulence at night. Second, canopy "greenness" changes the sizes of thermally-driven or "buoyant" turbulent eddies which often drive atmospheric mixing during the day. For example, dead vegetation with patches of bare soil will transfer the majority of adsorbed incoming solar radiation into buoyant thermal eddies which are highly efficient at mixing the atmosphere and reducing wind shear, while a green, photosynthetically active canopy will partition a significant amount of adsorbed radiation into evaporating water making less energy available to move upward as a buoyant eddy.

Over land, atmospheric mixing and its related flow characteristics have strong diurnal cycles forced by daytime heating and nighttime cooling of the surface. During daylight, a portion of incoming

radiation is absorbed by biomass and soil while the majority is transferred back to the atmosphere as sensible and latent heat. The magnitude of these energy fluxes is dependent on surface and near-surface soil moisture and canopy density which determines how much incoming radiation is partitioned into sensible heat (highly buoyant heat fluxes) and how much is transferred into latent heat or evapotranspiration (energy related to evaporating water from the vegetation and soil). Upward fluxes of sensible heat are the major producer of atmospheric mixing from the ground surface to the top of the boundary layer during the day and usually lead to reduced wind shear and more turbulent flows at wind turbine heights. Thus, understanding how the vegetative surface-atmosphere is coupled should lead to more accurate predictions of wind speed and turbulence in the rotor-disk.

Monthly average energy fluxes from the flux tower are shown in Figure 8. A positive heat flux shows net energy transferred from the surface to the atmosphere as a direct result of heating of the ground surface during daylight hours. It is assumed that energy fluxes at the flux tower are representative of conditions found along the ridgeline at the LIDARs. Although we observed small differences in air temperature and relative humidity between the two sites (Figures A12 and A13), vegetation, precipitation, and incoming radiation should not significantly change over the 1 km distance.

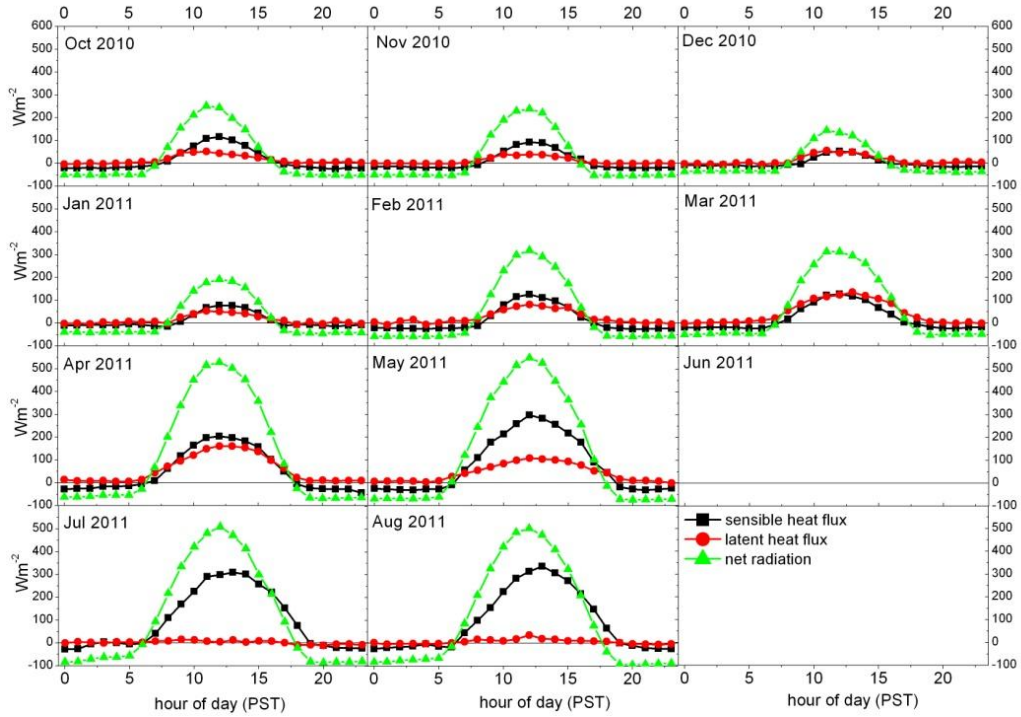

Figure 8: Monthly diurnal plots of energy exchange at the flux tower show how net radiation is partitioned into fluxes of sensible heat and latent heat at the grassland canopy. The monthly partitioning of energy is driven by changes in seasonal incoming radiation and canopy height, density, and "greenness". A smaller portion of incoming radiation is also transferred into the surface as ground heat storage (not shown here). Hence, the latent heat flux and sensible heat flux are not exactly 100% of net radiation.

The measurements in Figure 8 show that incoming radiation was evenly transferred into sensible heat and latent heat during the wetter months of December through April. This indicates that

nearly half of the incoming radiation was used to evaporate water from the canopy surface and soil and also to evaporate water from the plant tissue, i.e., stomatal water loss via transpiration. The wind profiles during this time exhibit positive shear during the day (Figures 5 and 6) indicating that the PBL was not moderately or strongly convective. As the canopy dried out and senesced in May (see Figure A1), a greater portion of incoming radiation was transferred into buoyant sensible heat fluxes, which should lead to increased atmospheric mixing and turbulence. By mid-summer, nearly all of the incoming radiation was transferred into buoyant heat fluxes as the surface was completely dry and the vegetative canopy was dead. Interestingly, the expected well mixed atmosphere was not visible during daytime hours in May-July and negative shear was observed instead (Figure 5). For reference, monthly changes in canopy vegetation "greenness" at the flux tower in FY11 are shown in Figure A1.

4. Conclusions

Complex terrain at Site 300 appears to strongly driving wind shear and turbulence so that it is not as dependent on surface energy fluxes as would a site in flat terrain. This suggests that a combination of surface-atmosphere energy exchange and terrain effects must be considered at Site 300 in order to understand and predict the wind power resource. In complex terrain, the impact of the energy budget on atmospheric mixing and rotor disk wind profiles is complicated by non-homogeneous advective wind flows. This complexity is directly applicable to the kinds of questions that could be investigated by developing Site 300 as a renewable energy testbed and are questions that continue to plague the American wind power industry. Usually wind turbines are sited along ridge lines with the assumption that these turbines will capture accelerated flow at heights equal to hub-height (~80 m) as the pressure fields converge on the windward side of hills. In reality such accelerations are expected only during near-neutral stability conditions and become increasingly complicated as the atmosphere becomes well mixed (i.e., convective) or as turbulence becomes suppressed (i.e., stable). Non-neutral stability affects wind flows by (1) changing the upwind velocity profile as predicted by similarity theory so that it is no longer logarithmic, and (2) changing flow characteristics above the surface layer (~ 100 m AGL) which in turn change the influence of a ridge line on the imposed pressure field. The observational network deployed and maintained for this SMS project found substantial changes in the expected wind field imposed by both complex terrain and localized surface-atmospheric heating. Maintaining these meteorological instruments is critical for validating forecasting models and for understanding the wind resource at Site 300 and will likely lead to future investments in renewable energy research at Site 300. For example, two LDRD proposals are currently pending for FY12 which will utilize these instruments and measurements for novel research in wind energy and atmospheric science.

Appendix: Additional Site 300 Figures

Figure A1: Photographs taken of the annual grassland canopy at the flux tower (elevation = 323 m). The photos show seasonal vegetation changes including a gradual greening up of the grasses in mid-winter, peak canopy height in April, and senescence in early summer through autumn. For reference, the LIDARs and tall meteorological tower are located along the ridge line in the background at an elevation of 385 m.

Figure A2: The project team downloading data from (left) the LIDAR co-located with the tall meteorological tower at the East Observational Point (EOP) and (right) the LIDAR near the lightning detector upwind of the flux tower. Both systems are fully equipped to run off of solar power. Elevations are 387 m, 387 m, and 398 m, respectively, for the tall meteorological tower, co-located LIDAR at the EOP, and the LIDAR near the lightning detector.

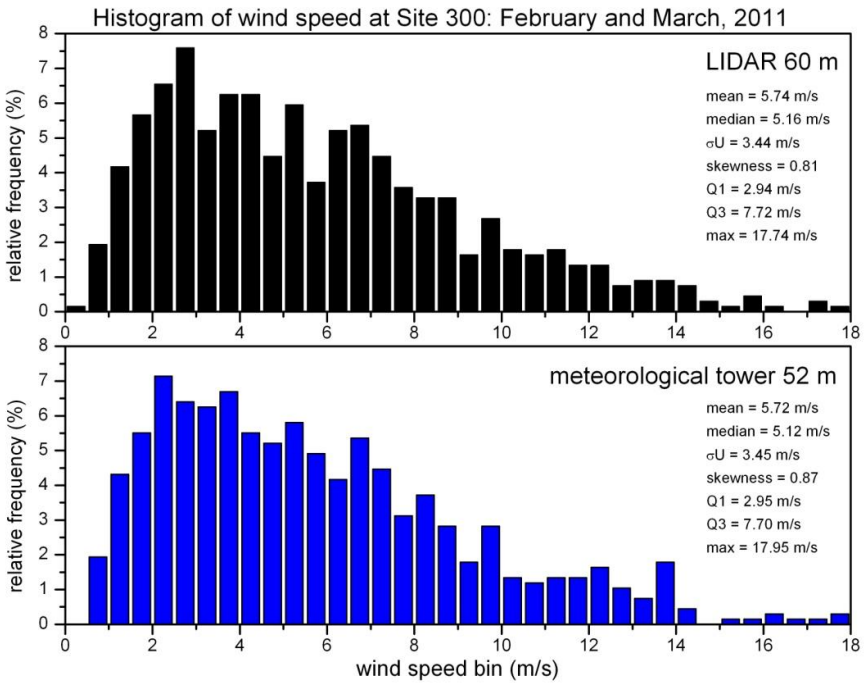

Figure A3: Comparison of hourly wind speeds measured by the LIDAR (60 m) and at the tall meteorological tower (52 m) for two months in 2011. The statistics show very good agreement between the two instruments.

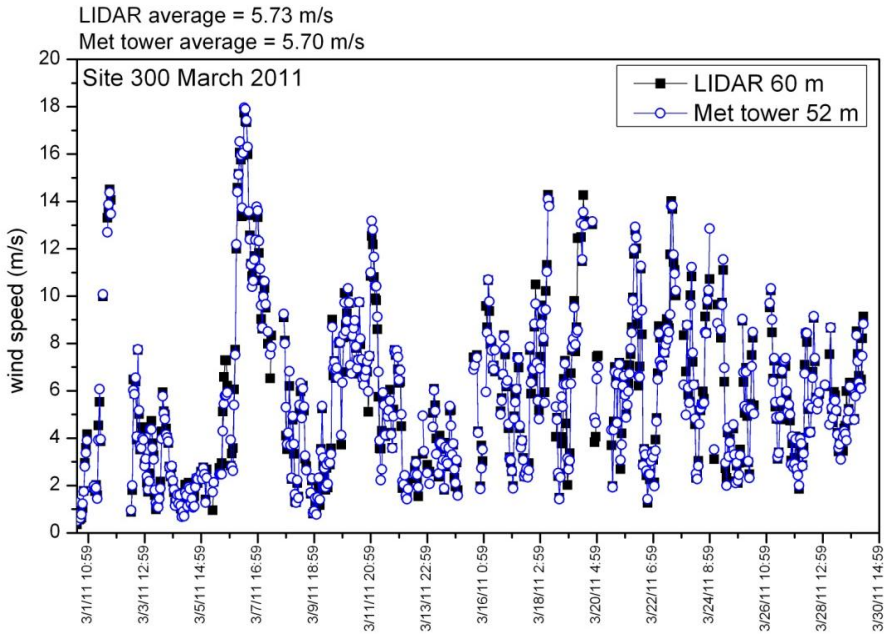

Figure A4: Time series of hourly wind speeds measured by the LIDAR (60 m) and the tall meteorological tower (52 m) for two weeks in March. The figure shows excellent agreement between the two instruments. Outliers are likely due to the instruments having slightly different averaging times which would produce slightly different averages, particularly during gusty periods.

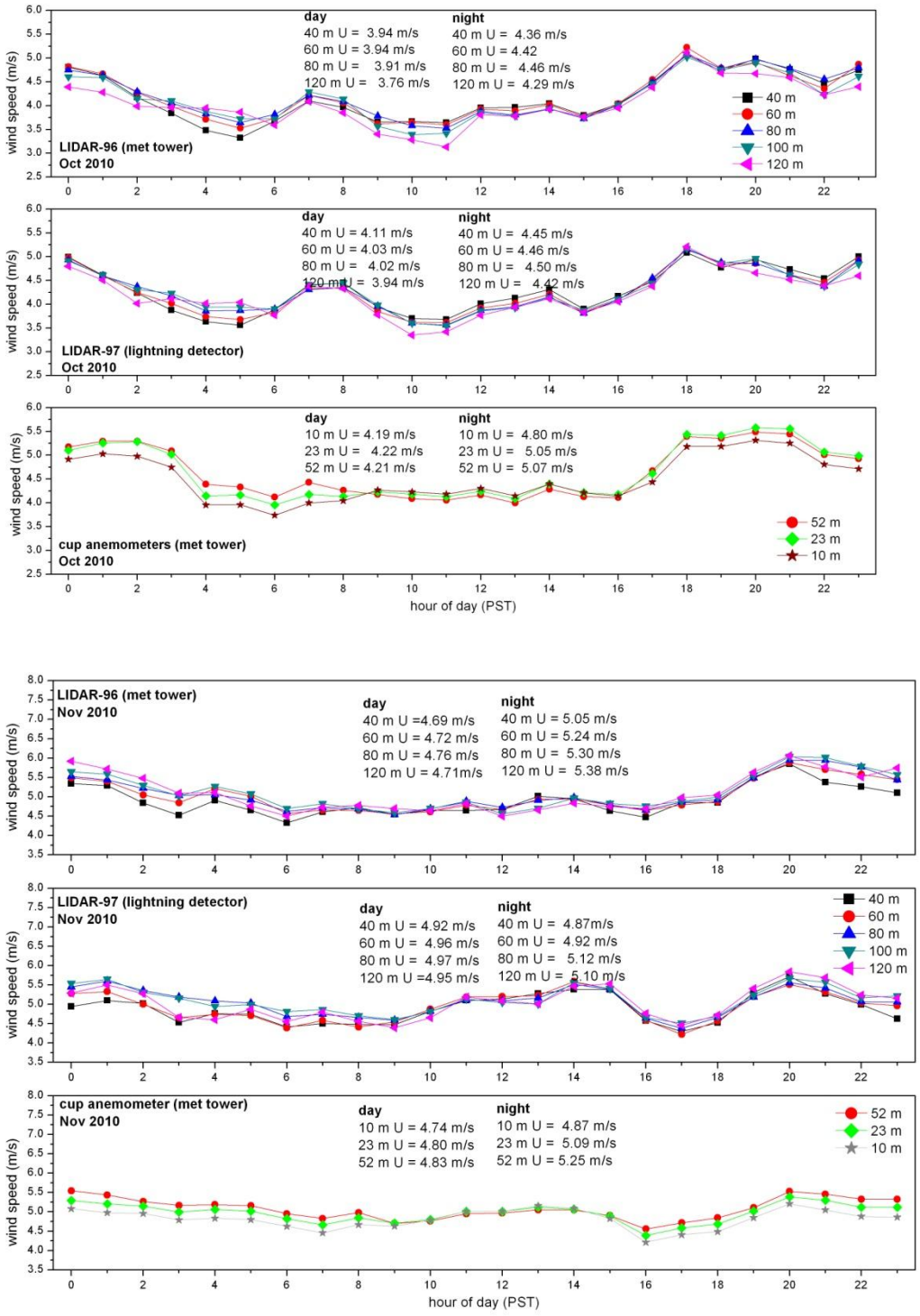

Figure A5: Monthly mean diurnal wind speeds in October (top) and November (bottom) 2010 at LIDAR-96, LIDAR-97, and the tall meteorological tower. During October and November, wind shear is larger at night than during the day and generally positive (i.e., wind speed increases with height). Note that heights 40 – 120 m are plotted for the LIDAR systems while the meteorological tower has measurements at 10, 23, and 52 m.

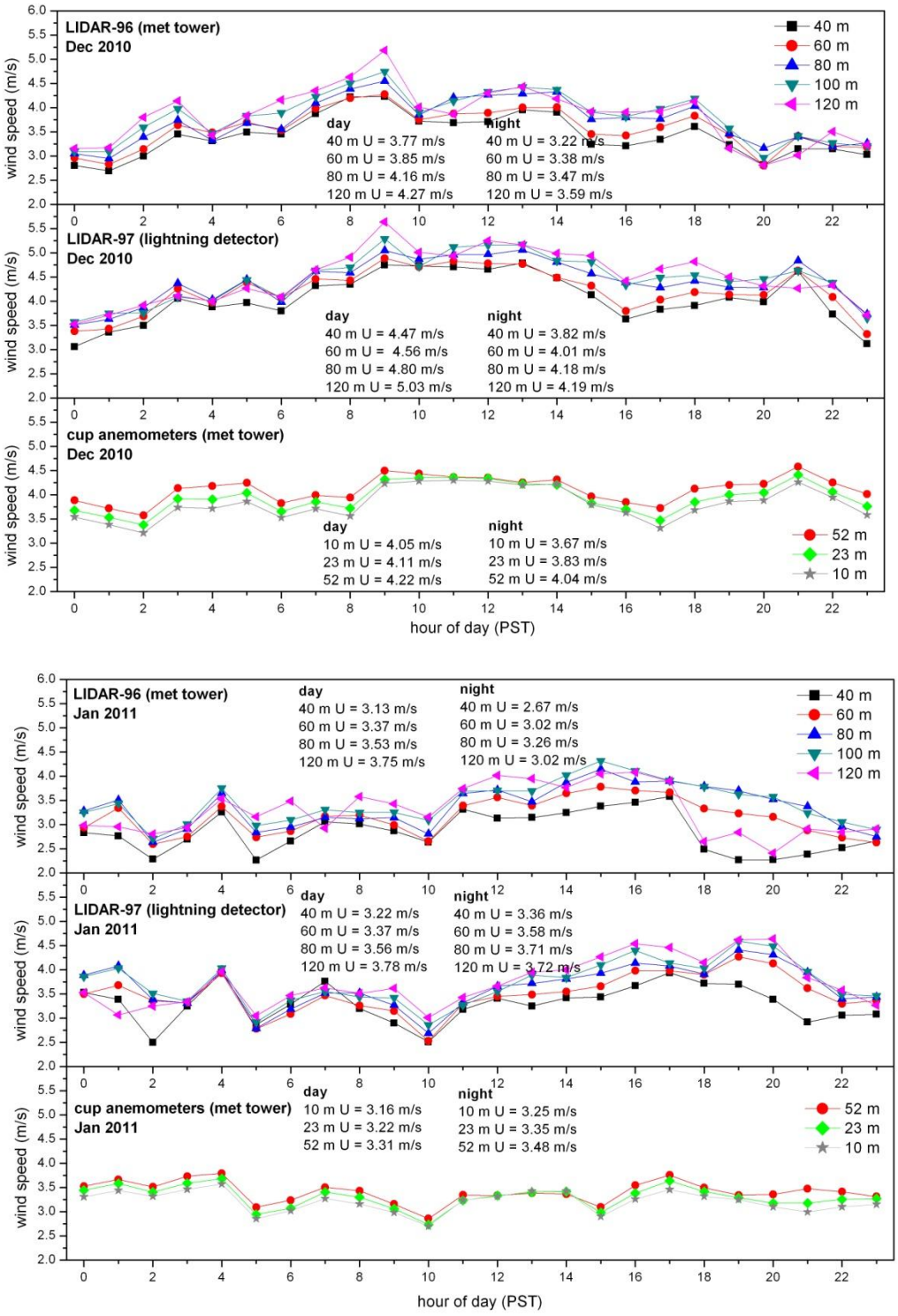

Figure A6: Monthly mean diurnal wind speeds in December 2010 (top) and January 2011 (bottom) at LIDAR-96, LIDAR-97, and the tall meteorological tower. During the winter months, wind shear is largest from hour 18 (6:00 PM PST) until hour 21 (9 PM PST) and is positive. Positive wind shear is observed during nearly every hour of the day. Note that the 120 m measurement height at LIDAR-96 may be underestimated during the nighttime hours because of lower data availability.

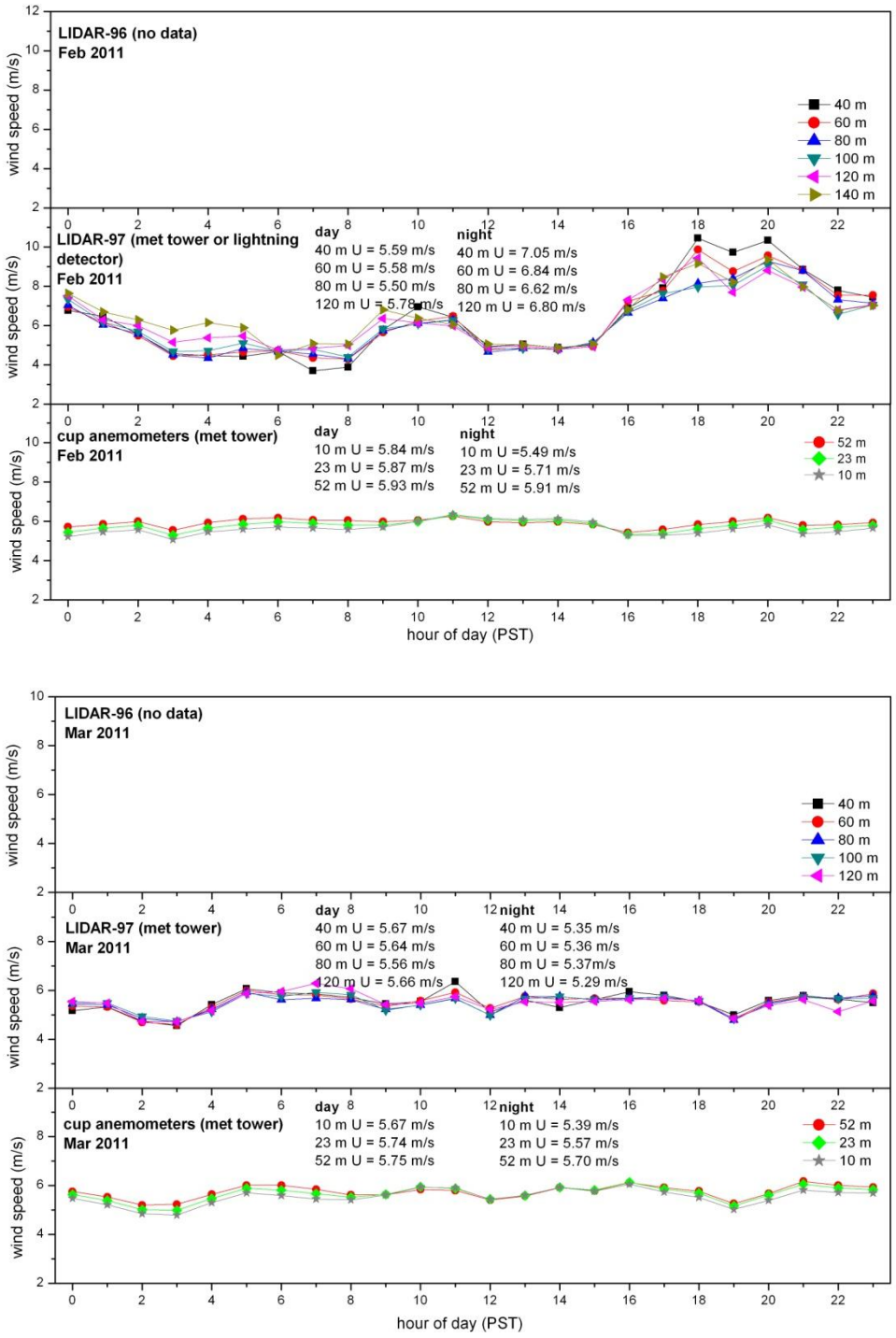

Figure A7: Monthly mean diurnal wind speeds in February (top) and March 2011 (bottom) at LIDAR-96, LIDAR-97, and the tall meteorological tower. LIDAR-96 data are missing because the unit went back to the manufacturer for software updates and repair. LIDAR-97 was moved to the meteorological tower in mid-February to ensure a complete data record at the EOP site. In February, wind shear is positive from midnight until 5 AM (PST) but is negative (i.e., wind speed is greatest at 40 m and decreases with height) from hour 18 (6:00 PM) until hour 22 (10:00 PM), coinciding with peak wind speeds. In March, in contrast, we observed very little diurnal differences in wind speed and very little wind shear.

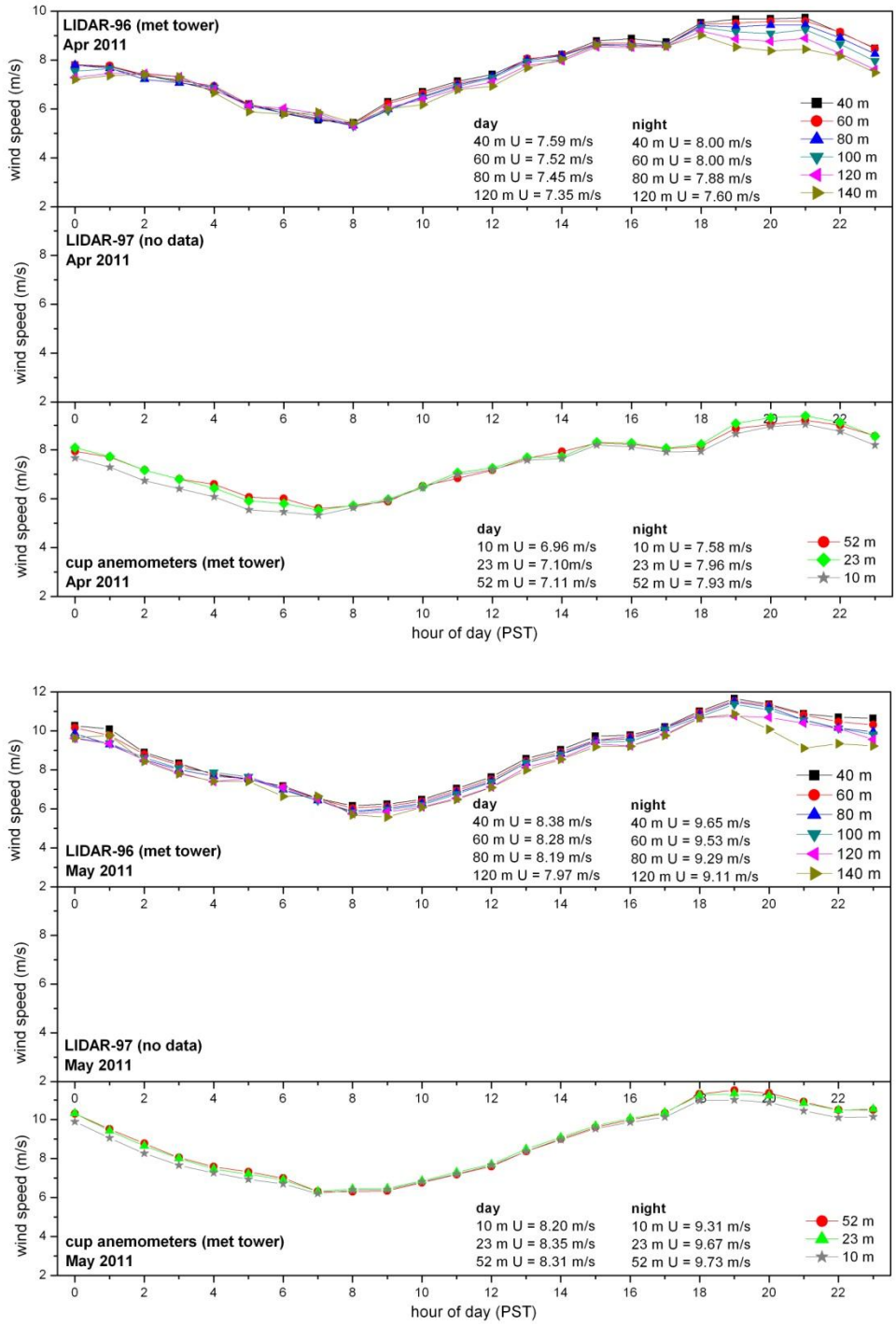

Figure A8: Monthly mean diurnal wind speeds in April (top) and May 2011 (bottom) at LIDAR-96, LIDAR-97, and the tall meteorological tower. LIDAR-97 data are missing because the unit was scheduled to return to the manufacturer for software updates. In April and May we observed distinct diurnal features with peak wind speeds around hour 19 (7:00 PM PST) and higher wind speeds over night than during the day. Minimum wind speeds were observed at hour 8 (8:00 AM PST). Wind shear was minimal except from hour 19 – 23 and was negative so that peak winds were at 40 m and minimal winds were at 140 m during these hours.

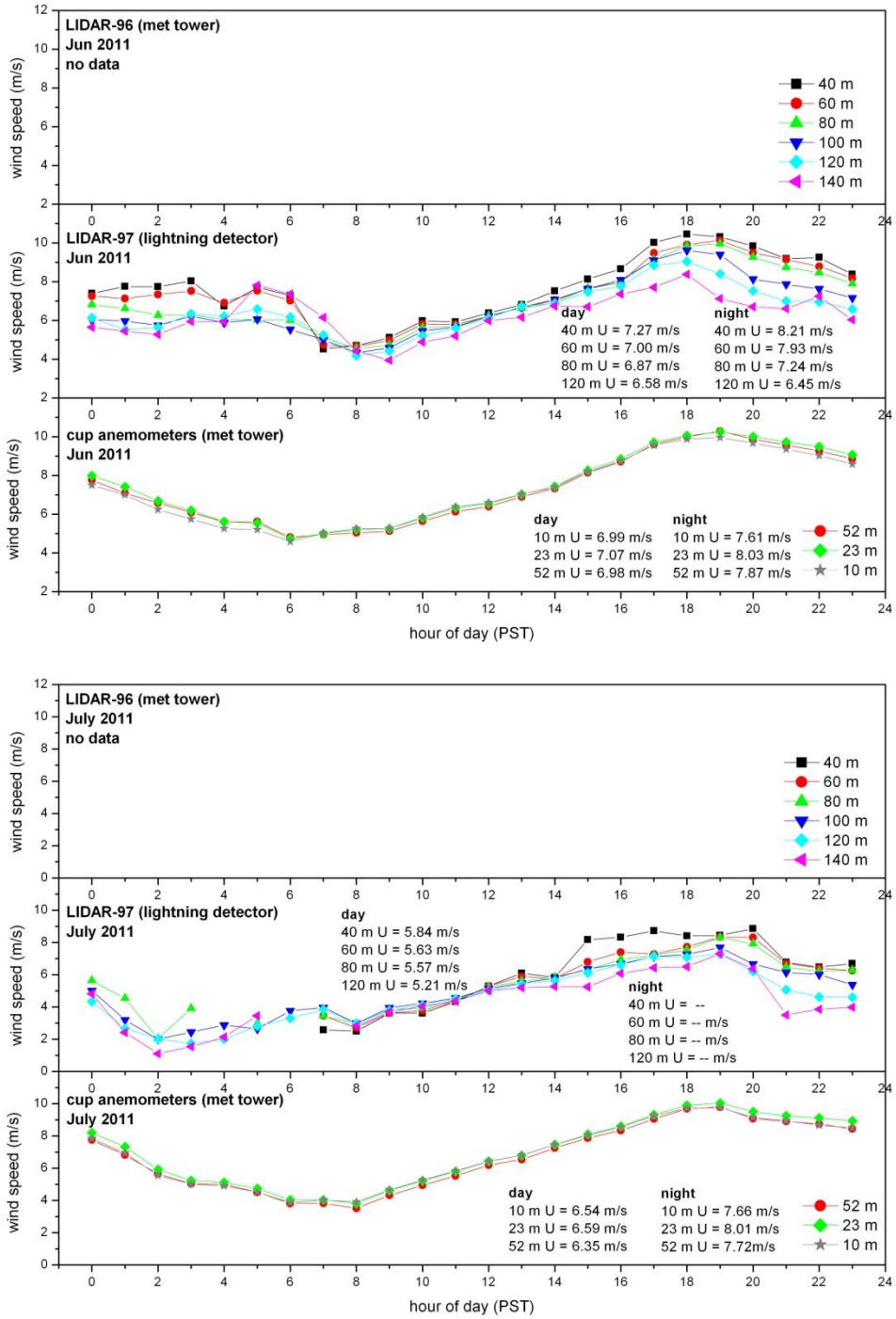

Figure A9: Monthly mean diurnal wind speeds in June (top) and July 2011 (bottom) at LIDAR-96, LIDAR-97, and the tall meteorological tower. LIDAR-96 data are missing because the unit was deployed in a DOE EERE wind forecasting project in South Dakota. In June and July wind shear is strongly negative during the nighttime hours and at night the 140 m wind speed is on average around 2 m/s lower than the 40 m wind speed. In July we started to see lower data recovery at the higher heights and during the nighttime hours. The signal to noise ratio has been steadily decreasing since June. The manufacturer stated that it appears to be an instrument issue and the unit will be returned to NRG for maintenance at the end of the fiscal year.

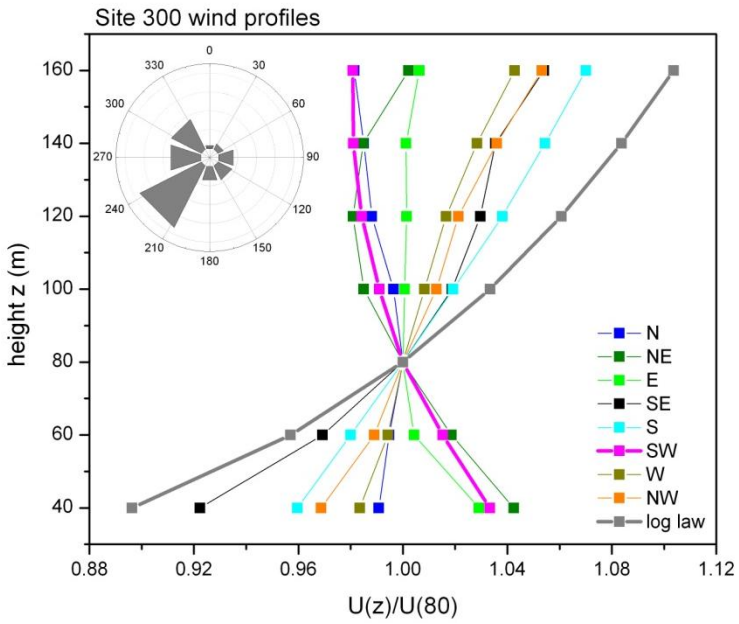

Figure A10: Vertical profiles of wind speed normalized by 80 m wind speed and as a function of wind direction at the EOP. The profiles were normalized by the 80 m observations (or typical hub-height) to illustrate if wind speeds in the top half of a wind rotor disk would be greater or less than hub-height and if wind speeds in the lower half of rotor disk would be greater or less than hub-height. Also plotted is the theoretical wind profile based on the log law. The wind shear observations appear to be highly dependent on wind direction. A negative wind speed profile is observed when winds are from the southwest, northeast, or east. The southwesterly wind direction is the most prevalent at the EOP ridgeline. Winds from the SW flow across areas of more complex terrain before reaching the EOP.

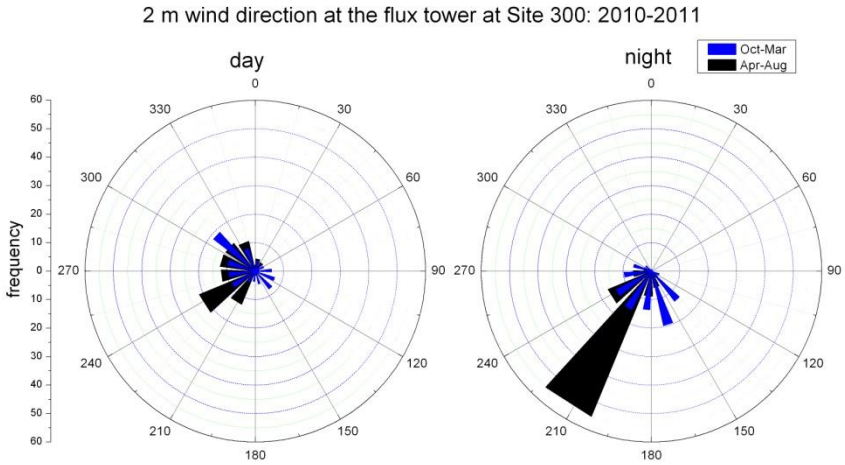

Figure A11: Histogram of (left) daytime and (right) nighttime wind direction by season at the flux tower. Daytime winds are more evenly distributed at the flux tower than along the ridge at the LIDARs during the daylight hours. Nighttime winds show a strong predominance in the south-southwesterly direction and show evidence of localized terrain effects as winds at the LIDAR at night are more southwesterly. LIDAR data for comparison are found in Figure 4.

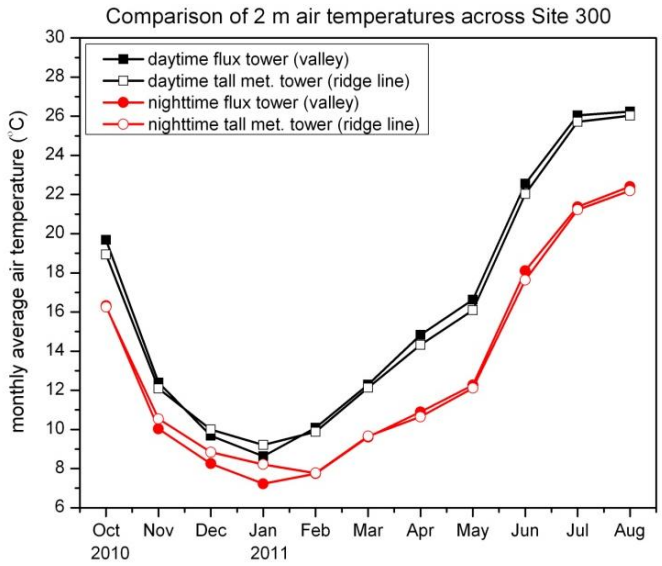

Figure A12: Monthly average air temperature at the flux tower and at the tall meteorological tower during daytime and nighttime periods. The flux tower is in a slight valley (323 m AGL) downwind of the higher elevation meteorological tower (387 m AGL). All measurements were taken at 2 m above the ground surface. It is apparent that the flux tower experiences localized temperature differences which are strongest during the winter months. On average, the flux tower experiences significantly colder nighttime temperatures during the winter months and warmer daytime temperatures during the spring and summer months.

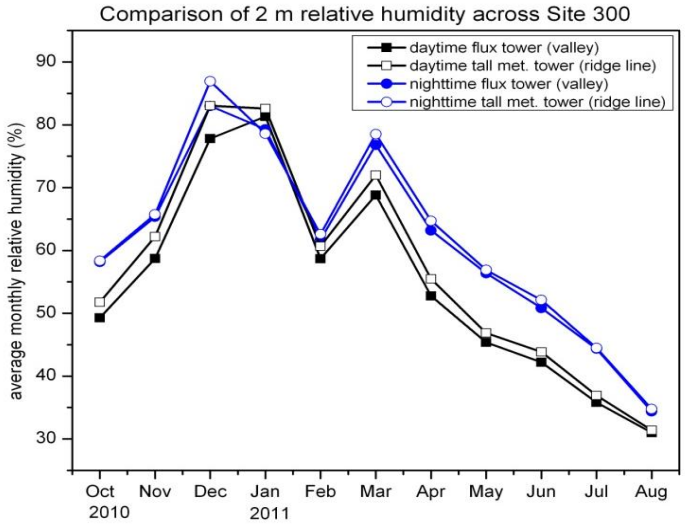

Figure A13: Monthly average relative humidity at the flux tower and tall meteorological tower during daytime and nighttime periods. All measurements were taken at 2 m above the ground surface. On average the flux tower location was drier than the ridge line, particularly during the daytime hours. Smaller differences were observed at night although the air above the valley is generally drier at night, too. Relative humidity differences suggest slight differences in canopy density (i.e., a denser, green canopy will have higher rates of transpiration), soil moisture, and/or localized differences in fog/low cloud cover (during the winter).